Polarity of anomalous Hall effect hysteresis loops in $[Pt/Co]_{15}/AF/[Co/Pt]_{15}$ (AF=FeMn, NiO) multilayers with perpendicular anisotropy

C. Christides[a)]
Department of Engineering Sciences, University of Patras, 26 504 Patras, Greece and Institute of Materials Science, NCSR "Demokritos", 153 10 Athens, Greece

Th. Speliotis
Institute of Materials Science, National Center for Scientific Research "Demokritos", 153 10 Athens, Greece

(Received 10 June 2004; accepted 30 September 2004; published online 13 December 2004)

The effect of the metallic antiferromagnet (AF) γ-FeMn and the AF-semiconductor NiO alloys on the polarity of anomalous Hall resistivity loops is examined in perpendicularly biased $[Pt(2\ nm)/Co(0.4\ nm)]_{15}/AF(3\ nm)/[Co(0.4\ nm)/Pt(2\ nm)]_{15}$ (AF=NiO, FeMn) multilayers. The Hall resistivity exhibits negative polarity for AF=NiO and positive polarity for AF=FeMn. These differences are explained by the reduced spin-diffusion-length effects and the specular reflection of electrons at FeMn and NiO interfaces, respectively. In addition, it is shown that a sandwiched AF thin layer stabilizes the exchange-bias effect via interlayer coupling between top $[Co(0.4\ nm)/Pt(2\ nm)]_{15}$ and bottom $[Pt(2\ nm)/Co(0.4\ nm)]_{15}$ structures in multilayers with strong perpendicular magnetic anisotropy.
 [DOI: 10.1063/1.1825628]

I. INTRODUCTION

Thin film Co/Pt multilayers that are exchange coupled with antiferromagnetic (AF) layers and exhibit perpendicular magnetic anisotropy (PMA) attract a growing interest of basic research[1–4] due to their potential use in magnetoelectronic devices.[5] In such systems the anomalous (extraordinary) Hall voltage V_H can be used as the output signal of the device[5] because the Hall resistivity is proportional to the perpendicular component ($M_\perp$) of magnetization[5,8,9]

$$\rho_H = \frac{V_H t_f}{I} = \rho_{xy} = R_0 H + R_s M_\perp, \tag{1}$$

where t_f is the film thickness, I is the electric current, H is the applied field, R_0 is the ordinary Hall coefficient, and R_s is the anomalous Hall coefficient (the demagnetization factor N is equal to 1 due to the geometry of the magnetic field H applied perpendicular to the film plane). Since, usually, the magnitude of the ordinary $|R_0 H|$ term is relatively small in metallic-polycrystalline films, the $|R_s M_\perp|$ term dominates the V_H signal for typical values of H. It is now accepted[6] that *skew-scattering* and *side-jump* mechanisms give different contributions to ρ_H. For bulk ferromagnets the skew-scattering contribution is proportional to longitudinal resistivity ρ_{xx} while both,[6] the skew-scattering and the side-jump mechanisms contribute to the quadratic ρ_{xx}^2 term, thus giving a simple expression of: $R_s = \alpha\rho_{xx} + \beta\rho_{xx}^2$. Recently, anomalous Hall effect (AHE) measurements in the ferromagnetic spinel[7] $CuCr_2Se_{4-x}Br_x$ have shown that the normalized AHE coefficient to the hole density, R_s/n_h, is proportional to ρ_{xx}^2 irrespective of the sign (polarity) of R_s. Based on this result Lee *et al.*[7] have argued that the same AHE (side-jump) mechanism occurs in both sign regimes. However, in view of the theoretical model of Crépieux and Bruno,[6] this is a false argument because the skew scattering mechanism, that is responsible for the linear term in R_s, should give also an important contribution to the quadratic term in the case of impurity scattering. This situation becomes more complex in heterogeneous systems, such as magnetic multilayers,[8–10] because the AHE is affected by other parameters than those present in the bulk.

The magnetotransport properties of magnetic multilayered structures are dominated by: (i) the scattering within layers that changes from one layer to another, (ii) the additional scattering resistivity due to the roughness of the interfaces between layers, and (iii) the resistivity that depends on the orientation of the magnetization of the magnetic layers. It has been shown theoretically[10] and experimentally[8,9,11] that interface scattering modifies the relationship between R_s and ρ_{xx} in multilayers. Specifically, it was found that the exponent of ρ_{xx} can be very different from 1 or 2 in[8] Co/Pt and[9] Co/Au multilayers with PMA when the ratio of Co layer thickness (t_{Co}) to nonmagnetic layer thickness (t_{NM}) is much less or much greater than one. These deviations have been attributed[8] to interface scattering, which seems to be the crucial mechanism[10] controlling the mean-free-path of the spin carriers in magnetic multilayers. The analysis of experimental data has shown[8] that the skew-scattering parameter $\alpha(\propto t_{Co})$ could be negative for $t_{Co}<1$ nm whereas the side-jump parameter $\beta(\propto 1/t_{Co})$ is dominated by interface scattering and thus, is insensitive to t_{NM}. In this context, it has been argued[8,12] that R_s depends on the relative magnitude and sign of α and β parameters in magnetic multilayers.

The present study investigates the effect of the metallic AF γ-FeMn and the AF-semiconductor NiO alloys on the R_s

[a)]Electronic mail: christides@des.upatras.gr

of perpendicularly biased $[Pt(2\ nm)/Co(0.4\ nm)]_{15}$/AF(3 nm)/$[Co(0.4\ nm)/Pt(2\ nm)]_{15}$ (AF=NiO, FeMn) multilayers.

II. EXPERIMENTAL DETAILS

$[Pt(2\ nm)/Co(0.4\ nm)]_{15}$/AF(3 nm)/$[Co(0.4\ nm)/Pt(2\ nm)]_{15}$ (AF=NiO or FeMn) multilayers were deposited onto thermally oxidized Si(001)/SiO_x(70 nm) substrates by dc and rf magnetron sputtering from separate targets in 3 mTorr Ar pressure. During deposition the temperature of the substrate has been kept close to RT by the water-cooled supporting table of copper. The AF targets were 99.95% pure, fcc γ-$Fe_{50}Mn_{50}$ or NiO compounds. NiO was directly deposited onto the sample,[2] without use of reactive sputtering. Both, the itinerant AF γ-$Fe_{50}Mn_{50}$, with the triple-Q structure,[13] and the AF-semiconductor[14] NiO alloys were deposited with a $t_{AF}=3$ nm in order to have a T_B below[3,15] RT. X-ray diffraction results show an average fcc Pt/Co structure where the (111) and (222) Bragg peaks appear closer to the *d*-spacing values of Pt, revealing strong (111)-texture. Isothermal magnetization and AHE loops were measured with a Quantum Design MPMSR2 superconducting quantum interference device magnetometer between 5 and 300 K. The samples were cooled from RT (which is above the T_B for the t_{AF} used) under a field of 6 kOe, applied perpendicular to the film surface. AHE measurements were performed with the van der Pauw method (see Fig. 1 in Ref. 16) using a dc current of 1 mA. All measurements were performed by first applying the maximum positive field $H=6$ kOe and then completing the loop.

III. EXPERIMENTAL RESULTS

Shown in Figs. 1 and 2 are Hall resistivity (solid line) and magnetization (open circles) hysteresis loops for the $[Pt(2\ nm)/Co(0.4\ nm)]_{15}$/AF(3 nm)/$[Co(0.4\ nm)/Pt(2\ nm)]_{15}$ multilayers, with AF=FeMn and NiO, respectively. There are two marked differences between the samples with AF=FeMn and NiO: (i) the polarity of ρ_H loops is negative for NiO (Fig. 2) whereas it becomes positive for FeMn (Fig. 1), (ii) the resistivity is larger when the AF-semiconductor NiO is used in the place of metallic γ-FeMn ($\rho_H \propto \rho_{xx}^n$). However, the hysteresis loops of magnetization exhibit similar features for AF=FeMn and NiO. These loops are typical of perpendicularly biased Co/Pt multilayers[4] where the reversal of magnetization is characterized by nucleation and domain wall motion before saturation. Starting from the saturated state (i.e., from a positive field of 6 kOe) the reversal process takes place by a rapid nucleation of domains at a well defined nucleation field H_n, resulting in the steep part of the hysteresis loop. The rapid drop in magnetization at H_n is followed by a sloped reversal behavior that persists up to the saturation field H_s, where the saturation magnetization $|M_s|$ is achieved. This behavior is symmetric to positive and negative fields, indicating that the evolution of the reverse domains is symmetric to positive and negative field sweeps.

An enhancement of coercivity is observed with decreasing field whereas a loop-shift towards negative fields appears below 30 K, evidencing a very low T_B relative to the Néel

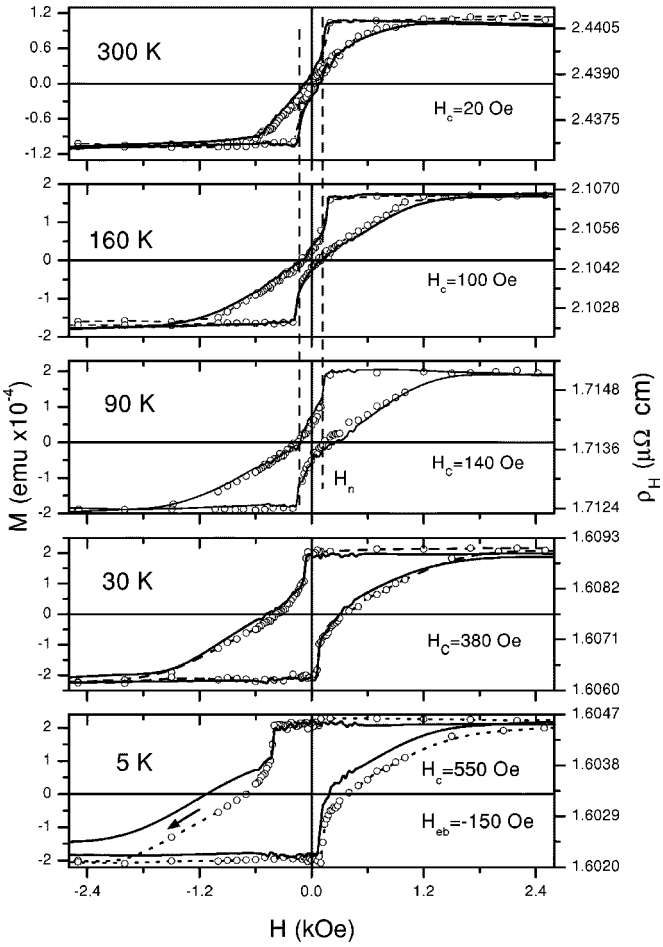

FIG. 1. AHE (line) and magnetization (circles) loops for $[Pt/Co]_{15}$/FeMn/$[Co/Pt]_{15}$ multilayers. The field is applied perpendicular to film plane. Dash lines mark the nucleation field H_n.

temperature T_N of 3 nm (about 12 monolayers) thick[17] FeMn ($T_N>$RT) or NiO ($T_N\simeq 400$ K, see Fig. 1 in Ref. 3) layers. Such a small T_B/T_N ratio can be explained from the competing anisotropies between the governing PMA in $[Co/Pt]_{15}$ sublayers and the weaker anisotropy of the AF layer used. Our results show that the PMA of the host (top and bottom) $[Co/Pt]_{15}$ sublayers (see Fig. 3) dominates the reversal mechanism of magnetization and the effect of the unidirectional anisotropy that comes from the inner Co/AF/Co interfaces becomes evident only at the very low temperatures. A comparison of the loops shown in Figs. 1 and 2 with those in Fig. 3 shows that the observed enhancement of H_c at lower temperatures does not arise from the interaction with the AF layers. Apparently the AHE and M–H loops exhibit the same coercive field H_c, indicating that, first, the easy axis of magnetization is perpendicular to film plane,[18] and second, the ρ_H follows the symmetric reversal of the domains. The shifted loops in Figs. 1 and 2 are symmetric about the exchange-bias field H_{eb}, as in perpendicular-biased $[Co(0.4\ nm)/Pt(0.7\ nm)]_4Co/CoO(1\ nm)$ multilayers.[4] Thus, the H_{eb} shifts the loop but it cannot alter the reversal pathway because the uniaxial anisotropy in Pt/Co interfaces is so strong that it limits potential reversal behavior.[4] Notice that the value of $H_{eb}=-150$ Oe is the same (Figs. 1 and 2) for AF=FeMn and NiO layers. This is an

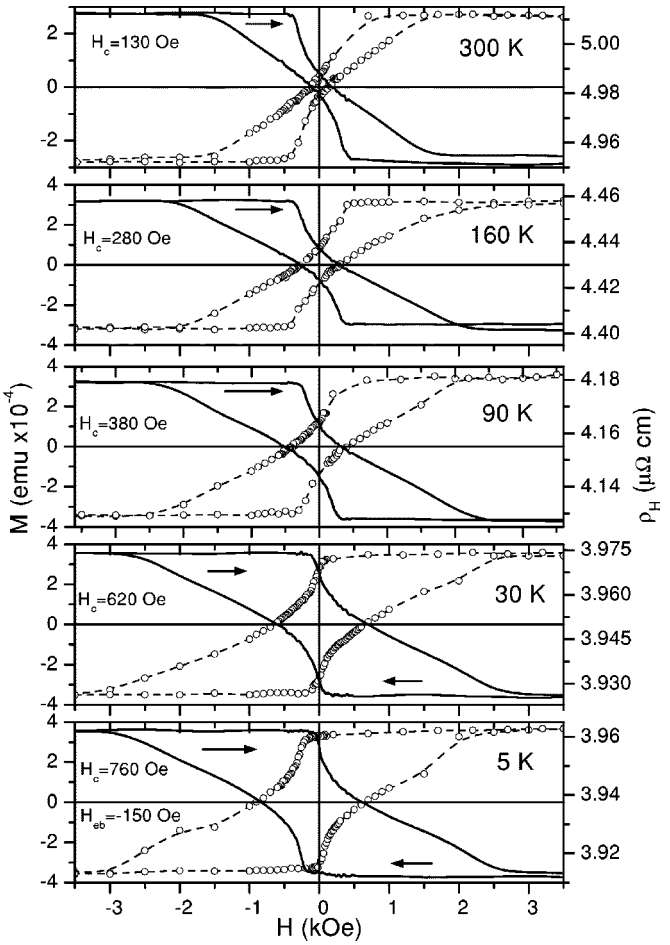

FIG. 2. AHE (line) and magnetization (circles) loops for $[Pt/Co]_{15}/NiO/[Co/Pt]_{15}$ multilayers. The field is applied perpendicular to film plane.

indirect evidence that the magnitude of H_{eb} depends predominantly[19] on the number of [Co/Pt] bilayer repeats and t_{AF} (which are the same in Figs. 1 and 2).

Shown in Fig. 3 are ρ_H (solid line) and magnetization (open circles) hysteresis loops for a $[Pt(2\ nm)/Co(0.4\ nm)]_{15}/Pt(2\ nm)$ multilayer. This figure shows that, first, the polarity of ρ_H loops is negative as in Fig. 2, and second, both kinds of loops do not mimic those observed in samples with sandwiched AF layers *at any temperature*. In contrast, it was observed[4] that the $[Co/Pt]_4$ sublayers respond collectively in perpendicularly biased $[Co(0.4\ nm)/Pt(0.7\ nm)]_4Co/CoO(1\ nm)$ and [Co(0.4 nm)/Pt(0.7 nm)]50 multilayers when the CoO layers are nonmagnetic at RT, as in the case of Co/Pt multilayers without the CoO layers. This difference can be attributed to the competition between the thermal activation energy and the energy barrier that is due to domain wall motion through the microstructure of the films, as explained in the discussion section later.

Figure 4 shows ρ_H hysteresis loops for a $[Pt(2\ nm)/Co(0.4\ nm)]_{15}/FeMn(3\ nm)/Pt(2\ nm)$ multilayer. Remarkably, the addition of a 3-nm-thick FeMn layer on top of $[Pt(2\ nm)/Co(0.4\ nm)]_{15}$ multilayers changes the polarity of R_s from negative (Fig. 3) to positive (Fig. 4). In addition, Fig. 4 shows that $H_{eb}=0$ between 5 and 300 K.

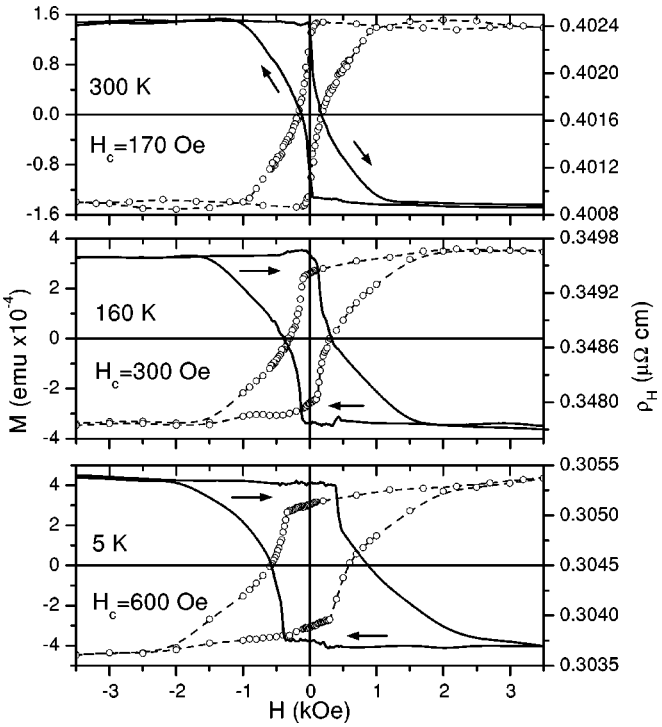

FIG. 3. AHE (line) and magnetization (circles) loops for $[Pt(2\ nm)/Co(0.4\ nm)]_{15}/Pt(2\ nm)$ multilayers. The field is applied perpendicular to film plane.

Note that similar measurements have shown a negative loop shift ($H_{eb}\neq 0$) when a 20-nm-thick FeMn layer was used. These results are reminiscent to those observed[19] in $[Pt(2\ nm)/CoFe(0.4\ nm)]_n/FeMn(x)/Pt(2\ nm)$ multilayers, indicating that the anisotropy of FeMn layers decreases as t_{AF} decreases.

However, the results in Fig. 1 show that addition of $[Co(0.4\ nm)/Pt(2\ nm)]_{15}$ sublayers onto [Pt(2 nm)/

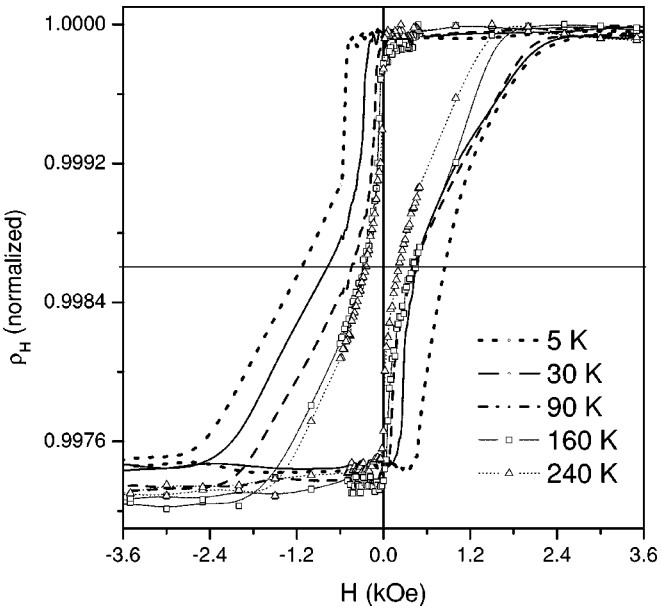

FIG. 4. Normalized AHE loops for $[Pt(2\ nm)/Co(0.4\ nm)]_{15}/FeMn(3\ nm)/Pt(2\ nm)$ multilayers. The field is applied perpendicular to film plane.

$Co(0.4\ nm)]_{15}/FeMn(3\ nm)$ multilayer stabilizes an $H_{eb}=-150$ Oe below 30 K. This is in contrast with the results reported in planar-exchange-biased FM1/AF/FM2 trilayers (FM1=NiFe, FM2=Co in Ref. 20 and FM1=Co, FM2=Co in Ref. 21), where the interaction between the FM1/AF exchange-biased system and the FM2 layer across the common AF=FeMn spacer eliminates the H_{eb} at the FeMn/FM2 interface. In such planar-exchange-biased[20] trilayers the highly randomized magnetic state of the top Co layers provides strong evidence for the random field model where an AF micromagnetic state that supports strong bias at the FM1/FeMn interface does not induce bias in a Co layer deposited on top. Our result (Figs. 1 and 4) shows the opposite case, where interlayer coupling between perpendicularly biased $[Pt/Co]_{15}$ sublayers across a common FeMn spacer favors the stabilization of a micromagnetic state in the AF which maintains exchange bias at low-temperatures when the simple $[Pt/Co]_{15}/FeMn$ structure does not exhibit exchange bias. This is in agreement with the results of Kuch *et al.*[17] in FM1/FeMn/FM2 trilayers *with identical easy axes of the* FM *layers*, which show that the FM1 and FM2 layers exhibit an oscillatory magnetic coupling between parallel and antiparallel alignment of the two FM layers across an FeMn spacer. In the case of a three-dimensional noncollinear AF phase in γ-FeMn layers it has been argued[17] that there are locally uncompensated inplane and out-of-plane AF-spin components which are exchange coupled with FM spins of the same component at the FM/AF interface, thus contributing to the exchange-bias (EB) effect above a certain FeMn layer thickness. In parallelism, the two FM $[Pt/Co]_{15}$ and $[Co/Pt]_{15}$ sublayers can be considered as the FM1 and FM2 layers of a FM1/FeMn/FM2 system *with out-of-plane* (identical) easy axes of the FM layers due to PMA from the Co/Pt interfaces, where interlayer coupling between the FM sublayer structures is established across an FeMn layer. Accordingly, the observed EB effect in Fig. 1 can be attributed to the *concerted action of exchange interactions* between locally uncompensated out-of-plane AF-spin components and Co spins of the same component at the top FeMn/Co and bottom Co/FeMn interfaces.

Figure 5 shows the temperature dependence of the resistance for all the Co/Pt-based samples and for a 70-nm-thick Pt film that is used as reference. The resistances, $R(T)$, were measured at zero field (ZF) between 5 and 320 K whereas an $H_{FC}=3$ kOe was applied perpendicular to film plane at 320 K and then the $R_{FC}(T)$ was measured in a field-cooling (FC) process. For each sample the $R(T)$ curves were normalized to the corresponding ZF resistance, $R_{ZF}(5\ K)$, of the same film at 5 K. Thus, the $R_{ZF}(5\ K)$ has been used as the residual resistance R_0 due to the temperature independent scattering from defects and impurities. In multilayers with AF=FeMn and NiO layers the $R_{FC}(T)$ data are above the corresponding $R_{ZF}(T)$ measurements at lower temperatures. In this case the $R_{FC}(T)$ values below 50 K tend to FC residual resistances which are about 2%–3% higher than the corresponding ZF resistances. It can be considered as the manifestation of the exchange bias effect which is expected[22] to modify the asymmetric scattering of the conduction electrons in the Co/Pt layers that are responsible for the AHE. In

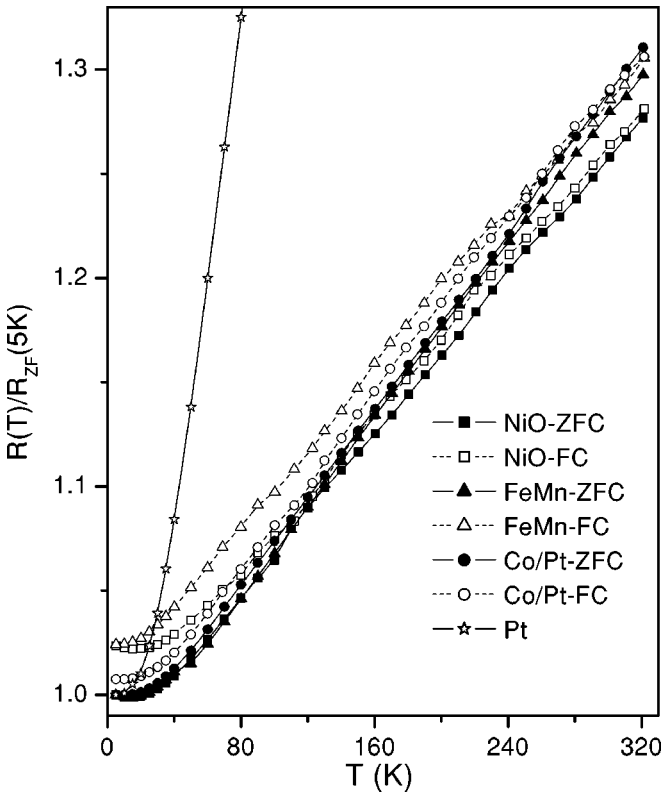

FIG. 5. Typical temperature dependence of the resistance: Normalized ZF (black symbols) and FC (open symbols) $R(T)$ measurements for $[Pt(2\ nm)/Co(0.4\ nm)]_{15}/AF(3\ nm)/[Co(0.4\ nm)/Pt(2\ nm)]_{15}]$ (AF=NiO →squares, FeMn→triangles), $[Pt(2\ nm)/Co(0.4\ nm)]_{15}/Pt(2\ nm)$ (circles) multilayers and 70-nm- thick Pt film. $H_{FC}=3$ kOe, applied perpendicular to film plane. Lines are guides to the eye.

agreement, no difference is observed between ZF and FC $R(T)$ curves for the $[Pt(2\ nm)/Co(0.4\ nm)]_{15}/Pt(2\ nm)$ and $[Pt(2\ nm)/Co(0.4\ nm)]_{15}/AF(3\ nm)/Pt(2\ nm)$ multilayers that do not exhibit EB. Since at $H_{FC}=3$ kOe the magnetization of all these films is saturated, magnetic scattering contributions[23] should be taken into account as well. They arise from the exchange interaction between the conduction electrons (s) and the localized 3d electrons (called *$s-d$ interaction*). It has been observed[23] that the temperature dependence of electrical resistance in magnetically saturated (FM state) Fe/Cr multilayers below 15 K is better described by

$$R(T) = R_0 + A\left(\frac{T}{\theta_D}\right)^n \int_0^{\theta_D/T} \frac{z^n dz}{(e^z-1)(1-e^{-z})} + \kappa T^2, \qquad (2)$$

where the second term gives the relative contribution from electron-phonon assisted interband *$s-d$ scattering* when $n=3$ in the low-temperature limit or the classical linear increase in the high-temperature limit:[24] $R \propto T$ ($n=1$), θ_D is the Debye temperature, the third term is the magnetic contribution[23] from the *$s-d$ interaction* (not *$s-d$ scattering*) and κ includes its strength. Least square fits of the $R(T)$ data of pure Pt below 60 K with the function: $R(T)=R_0+\kappa T^n$, give the parameters: $R_0=0.0813(2)\Omega$, $\kappa=2.4(8)\mu\Omega K^{-2}$, and $n=2.1(1)$, evidencing the dominance of the T^2 law (*$s-d$ interaction*) at low temperatures. As seen in Fig. 5, the main effect of Co layers into $R(T)$ of pure Pt is to decrease the $\Delta\rho/\Delta T$ rate in the quasilinear part of R vs T data. The ZF

and FC $R(T)$ of the multilayers fits to the function: $R(T) = R_0 + \kappa T^n$ below 60 K, giving least-square best estimates for the exponent n that are close to 2.0(1) in the case of AF = FeMn and $[Co/Pt]_{15}$ films whereas for AF = NiO the n equals to 2.8(1). The latter shows a dominance of the T^3 law ($s-d$ electron-phonon scattering) over the T^2 law (electron-magnon scattering) at low temperatures which can be explained from the specular reflection of the spin-up and spin-down currents at NiO/Co interfaces.[25,26] Parenthetically we note that a reduced giant-magnetoresistance ratio in FeMn-based spin valves can also (partially) be understood[26] if spin-flip (magnon) scattering is present in the antiferromagnetic part of the stack, which is obviously absent in the case of the impenetrable NiO. Since electron-magnon scattering gives[23,24] a T^2 dependence in $R(T)$ at low temperatures then the dominance of the T^3 term in the $R(T)$ of Co/Pt multilayers with an AF = NiO layer indicates that electron reflectivity at NiO/Co interfaces reduces the effect of elecron-magnon scattering (*$s-d$ interaction*) and, as the temperature drops, the relative contribution from electron-phonon scattering increases.[24] However, the accuracy of our dc-resistivity measurements is not adequate to resolve reliably the relative contributions from the second and third terms in Eq. (2) at low-temperatures. Finally, Fig. 5 shows that above 60 K the $R(T)$ exhibits a quasilinear dependence on T, as in Ref. 22.

IV. DISCUSSION

The most important result of this study is the induced change of the AHE loop polarities by addition of a very thin FeMn metallic layer. The AHE loops in Figs. 1–4 reveal that the change of the polarity of ρ_H loops with addition of a thin FeMn layer *does not depend on*: (i) *the presence of EB effect* and (ii) *the position of the FeMn layer in the stacking sequence* of Co/Pt multilayers. To understand this effect we have to write the expression for the total Hall resistivity as[27]

$$\rho_H = \rho_{xy} \simeq -\lambda_{so} M_\perp (A\rho_{xx} + B\rho_{xx}^2) + CJ^3\chi_0, \tag{3}$$

where λ_{so} is the spin-orbit coupling constant, A and B are constants that their signs depend on the position of the Fermi level in a band,[28,29] C is a positive parameter, J is the exchange coupling integral that is positive if the interaction is the $s-d$ exchange, and $\chi_0 \propto \chi_{ijk} = \mathbf{S}_i \cdot (\mathbf{S}_j \times \mathbf{S}_k)$ is the total (uniform) chirality that is proportional to the scalar spin chirality χ_{ijk}. The last term in Eq. (3) has been introduced because chirality-driven AHE contributions might be observed[13] in the three-dimensional noncollinear AF spin structure[17] of γ-FeMn due to lattice distortions perpendicular to (111) plane.[13]

In FM/NM multilayers there are very few cases where a reversal of AHE loop polarity from positive to negative has been reported. This has been observed in Pd/Co multilayers[30] with monoatomic Co layer as a function of the number of Pd monolayers whereas in Co/Bi multilayers,[12] with fixed Co and Bi layer thicknesses, the polarity of the AHE loops changes progressively from positive at ambient conditions to negative below 140 K. In Pd/Co multilayers these results have been explained[30] from the strong dependence of A and B parameters [Eq. (3)] on the position of the Fermi level. It has been argued that[30] a shift of the Fermi level by increasing the layer thickness of Pd changes the relative population of the charge carriers (from hole-like to electron-like) and, thus, reverses the polarity of the AHE loops. In Co/Bi multilayers[12] the change of AHE polarity with temperature might be explained from a change in the sign of λ_{so} that could happen whenever a Fermi surface[31] crosses Brillouin zone boundaries, special symmetry points or lines of accidental degeneracy. In view of these two physical mechanisms it is rather surprising that a 3-nm-thick FeMn layer reverses the polarity of AHE loops, since it is most unlikely to disturb the sign of λ_{so} or the position of the Fermi level throughout the much thicker, $[Pt/Co]_{15}$ sublayer structures used in Figs. 1 and 4.

Usually, Co/Pt multilayers with PMA exhibit[32,33] negative polarities in ρ_H loops, as in Fig. 3. Electronic band structure calculations for Co/Pt interfaces indicate[34] that the electronic states at the bottom of the valence band are formed mainly by Pt states while the states in the vicinity of the Fermi level have predominantly Co 3d character with an admixture of Pt d states. Thus, the sign of the conducting charge carriers depends on a sensitive way from the degree of hybridization between the exchange-splitted Co 3d and Pt d states at the interface. AHE loops[32,33] (Figs. 2 and 3) evidence a negative polarity for thick enough Pt layers, as in Co/Pd multilayers.[30] Total density of states calculations (TDOS) for γ-$Fe_{0.5}Mn_{0.5}$ indicate that[35] its TDOS is similar to that of fcc Mn in the examined lattice constant range (0.33–0.39 nm). In the case of AF γ-$Fe_{0.5}Mn_{0.5}$ the DOS for the spin majority and minority bands of Fe and Mn are split in a way that the moment of each spin is equal but opposite to each other.[35] However, if one considers the two sublattice model for metallic γ-$Fe_{0.5}Mn_{0.5}$ then the AHE conductivity σ_{xy} should be zero.[13]

Theoretically, the only way to observe a $V_H \neq 0$ signal in AF γ-$Fe_{0.5}Mn_{0.5}$ is when the three-dimensional noncollinear AF spin structure[17] of fcc FeMn is distorted perpendicular to (111) plane.[13] According to this model the observed (Figs. 1 and 4) reversal of polarity in ρ_H loops can be attributed to current shunting through the 3-nm-thick FeMn layer. Thus, to explain the reversal of AHE polarity in Figs. 1 and 4 we have to assume that current shunting gives rise to a positive ρ_H contribution via the last term of Eq. (3) that surpasses the negative ρ_H contribution (Fig. 3) from the Co/Pt multilayer in the first term of Eq. (3). This is also consistent with the observed (Figs. 1 and 4) independence of the polarity of ρ_H loops from the presence of the EB effect and the position of the FeMn layer in the stacking sequence of Co/Pt multilayers when a thin FeMn layer is added. Furthermore, one may argue that even without reflectivity of electrons at Co/NiO interfaces the impenetrable (insulating) NiO layer prevents any shunting of current through subsidiary layers (such as FeMn in the metallic case) and it does not affect the negative polarity of ρ_H loops in Fig. 2. However, if the last term of Eq. (3) had such a large contribution to ρ_H then a significant AHE would be observed in pure FeMn thin films. This is not reported in the literature and we could not detect an AHE signal in FeMn thin films as well. It shows that the positive polarity in Figs. 1 and 4 results from a combination of resis-

tivity effects in both, the Co/Pt multilayer and the AF FeMn layer. Such an effect may arise from the very short spin-diffusion length,[36] $l_{sf} \approx 1.5$ nm, of FeMn layers in a multilayered structure. Thus, it can be argued that spin-memory loss at FeMn interfaces reduces the mean-free-path of the conducting spin-channels in Co/Pt layers whereas electron reflectivity at NiO interfaces it does not. The former can change the relaxation times $t_{\uparrow,\downarrow}$ of majority and minority electrons in Co/Pt layers but the second cannot do that. Since, generally, l_{sf} could be different for spin-up and spin-down channels then FeMn interfaces provide another spin-orbit scattering potential V_{so} at the interfaces that, in principle, can alter the relative contribution of the spin carriers which participate in the AHE of Co/Pt multilayers. This might be a more reasonable explanation for the change of AHE loop polarities in Figs. 1–4.

Another important feature of the loops in Figs. 1–4 is the temperature dependence of H_c and H_n fields on the kind of AF layer used. Specifically, Figs. 1 and 2 reveal that the magnitudes of H_n are different between AF=FeMn and NiO layer. Such differences in $|H_n|$ can be attributed to different grain size distributions[37,38] in these structures. Indeed, computer simulations for the dependence of magnetization reversal on the crystallite size[37] have shown that the larger the average grain size the smaller is expected to be the $|H_n|$ in thin films with PMA. In addition, positive H_n values appear in the positive field branch of a loop above 30 K. Specifically, the H_n shifts from −400(−200) Oe at 5 K to −40(+40) Oe at 30 K to +200(+400) Oe at 90, 160, and 300 K for AF=FeMn(NiO), giving a $\Delta H_n = |H_n(5\text{ K}) - H_n(300\text{ K})| = 600$ Oe in both cases. Such positive H_n features are reminiscent to a singularity of the M vs H curve that appears at some point H_0 in perpendicularly magnetized Co thin films.[39] This singularity has been ascribed to a sudden nucleation of magnetic bubbles with opposite magnetization[39] due to the existence of a critical bubble radius $R_0(H_0)$ under which a bubble network does not form a stable configuration. However, the magnitude of H_n is much lower in our case than that of $H_0(\approx 12$ kOe) in Ref. 39 because the PMA in Co/Pt multilayers with very thin Co layers comes mainly from (weaker) interface contributions to magnetic anisotropy[40,41] whereas in epitaxial Co films it comes from the (strongest) uniaxial anisotropy of the hexagonal (hcp) lattice. Thus, the observed loop shapes in Figs. 1–4 indicate that the domain structure in our multilayers is dominated by the same magnetic energy terms as in CoPt thin films[38] with PMA. The main difference between our Co/Pt multilayers and the CoPt alloy films is that interface anisotropy gives rise to PMA in fcc-modulated Co/Pt multilayers instead of uniaxial anisotropy in CoPt alloys. Since this factor does not contribute in the micromagnetic modeling[38] of CoPt alloy films, then the conclusions of Nowak *et al.*[38] can be applied in our case as well. These results show[38] that the hysteresis in CoPt thin films can be described as a depinning transition of the domain walls. For finite temperatures this transition is rounded by thermal activation and for fields smaller than the depinning field the domain wall movement is dominated by thermal activation.[38] In accordance, the observed temperature dependence of the hysteresis loops in Figs. 1–4 can be explained from the competition between the thermal activation energy and the energy barrier that is due to domain wall motion through the grains.[38]

V. SUMMARY

In summary, the effect of AF γ-FeMn (metallic) and insulating NiO layers on the polarity of AHE loops of Co/Pt multilayers with PMA has been studied. It was shown that $[\text{Pt}(2\text{ nm})/\text{Co}(0.4\text{ nm})]_{15}/\text{AF}(3\text{ nm})/[\text{Co}(0.4\text{ nm})/\text{Pt}(2\text{ nm})]_{15}$ (AF=NiO, FeMn) multilayers exhibit a negative polarity of ρ_H loops for AF=NiO whereas a change of polarity has been observed for AF=FeMn. The AHE loops in Figs. 1–4 reveal that the change of the polarity of ρ_H loops with addition of a 3-nm-thick FeMn layer does not dependent on, first, the presence of EB effect and, second, the position of the FeMn layer in the stacking sequence of Co/Pt multilayers. This can be explained from the very short l_{sf} of spin-up and spin-down channels in FeMn interfaces which modifies the spin-relaxation times $t_{\uparrow,\downarrow}$ in Co/Pt and, thus, might change the relative contribution of the spin carriers that participate in the AHE of Co/Pt multilayers. Figure 1 shows that $H_{eb} \neq 0$ at 5 K whereas $H_{eb}=0$ at all temperatures in Fig. 4. This difference provides an indirect evidence for interlayer coupling between perpendicularly biased $[\text{Pt/Co}]_{15}$ sublayers across a common AF spacer that causes an $H_{eb} \neq 0$ at 5 K in Figs. 1 and 2 whereas the simple $[\text{Pt/Co}]_{15}/\text{FeMn}(3\text{ nm})$ structure (Fig. 4) does not exhibit exchange bias. However, exchange-biased FM1/FeMn/FM2 trilayers[20,21] with in-plane magnetization exhibit a very different behavior. Their interaction between the FM1/FeMn exchange-biased system and the FM2 layer across the common FeMn spacer eliminates[20,21] the H_{eb} at the FeMn/FM2 interface. Such a difference between perpendicularly-biased and in-plane biased FM1/FeMn/FM2 structures indicates that EB is stabilized in a sandwiched AF thin layer[2,17] via interlayer coupling between top and bottom FM layers with PMA.

[1] F. Garcia, J. Sort, B. Rodmacq, S. Auffret, and B. Dieny, Appl. Phys. Lett. **83**, 3537 (2003).
[2] Z. Y. Liu and S. Adenwalla, Phys. Rev. Lett. **91**, 037207 (2003).
[3] Z. Y. Liu and S. Adenwalla, J. Appl. Phys. **94**, 1105 (2003).
[4] O. Hellwig, S. Maat, J. B. Kortright, and E. E. Fullerton, Phys. Rev. B **65**, 144418 (2002).
[5] F. Garcia, F. Fettar, S. Auffret, B. Rodmacq, and B. Dieny, J. Appl. Phys. **93**, 8397 (2003).
[6] A. Crepieux and P. Bruno, Phys. Rev. B **64**, 014416 (2001); Y. Yao, L. Kleinman, A. H. MacDonald, J. Sinova, T. Jungwirth, D. Wang, E. Wang, and Q. Niu, Phys. Rev. Lett. **92**, 037204 (2004).
[7] W.-L. Lee, S. Watauchi, V. L. Miller, R. J. Cava, and N. P. Ong, Science **303**, 1647 (2004).
[8] C. L. Canedy, X. W. Li, and G. Xiao, Phys. Rev. B **62**, 508 (2000).
[9] W. Vavra, C. H. Lee, F. J. Lamelas, H. He, R. Clarke, and C. Uher, Phys. Rev. B **42**, 4889 (1990).
[10] S. Zhang, Phys. Rev. B **51**, 3632 (1995).
[11] V. Koreviniski, K. V. Rao, J. Kolino, and I. K. Schuller, Phys. Rev. B **53**, R11938 (1996).
[12] S. Honda and Y. Nagata, J. Appl. Phys. **93**, 5541 (2003).
[13] R. Shindou and N. Nagaosa, Phys. Rev. Lett. **87**, 116801 (2001).
[14] G. A. Savatzky and J. W. Allen, Phys. Rev. Lett. **53**, 2339 (1984).
[15] W. J. Antel, Jr., F. Perjeru, and G. R. Harp, Phys. Rev. Lett. **83**, 1439 (1999).
[16] T. R. McGuire, R. J. Cambino, and R. C. Taylor, J. Appl. Phys. **48**, 2965 (1977).
[17] W. Kuch, L. I. Chelaru, F. Offi, J. Wang, M. Kotsugi, and J. Kirschner,

Phys. Rev. Lett. **92**, 017201 (2004).
[18]D. G. Stinson, A. C. Palumpo, B. Brandt, and M. Berger, J. Appl. Phys. **61**, 3816 (1987).
[19]F. Garcia, G. Casali, S. Auffret, B. Rodmacq, and B. Dieny, J. Appl. Phys. **91**, 6905 (2002).
[20]C. W. Leung and M. G. Blamire, J. Appl. Phys. **94**, 7373 (2003).
[21]F. Matthes, A. Rzhevskii, L.-N. Tong, L. Malkinski, Z. Celinski, and C. M. Schneider, J. Appl. Phys. **93**, 6504 (2003).
[22]J. L. Menéndez, D. Ravelosona, and C. Chappert, J. Appl. Phys. **95**, 6726 (2004).
[23]R. S. Patel, A. K. Majumda, A. F. Hebard, and D. Temple, J. Appl. Phys. **93**, 7684 (2003).
[24]B. G. Almeida, V. S. Amaral, J. B. Sousa, R. Colino, I. K. Schuller, V. V. Moschalkov, and Y. Bruynseraede, J. Appl. Phys. **85**, 4433 (1999).
[25]W. F. Egelhoff *et al.*, J. Appl. Phys. **78**, 273 (1995).
[26]H. J. M. Swagten, G. J. Strijkers, P. J. H. Bloemen, M. M. H. Willekens, and W. J. M. de Jonge, Phys. Rev. B **53**, 9108 (1996).
[27]G. Tatara and H. Kawamura, J. Phys. Soc. Jpn. **71**, 2613 (2002).
[28]E. I. Kondorskii, Sov. Phys. JETP **28**, 291 (1969).
[29]C. L. Chien and C. R. Westgate, *The Hall Effect and Its Application* (Plenum, New York, 1980), pp. 55–76.
[30]S. Kim, S.-R. Lee, and J.-D. Chung, J. Appl. Phys. **73**, 6344 (1993).
[31]J. Fabian and S. D. Sarma, Phys. Rev. Lett. **81**, 5624 (1998).
[32]R. A. Hajjar, M. Mansuripur, and H.-P. D. Shieh, J. Appl. Phys. **69**, 7067 (1991).
[33]T.-H. Wu, J. C. A. Huang, L. C. Wu, L. X. Ye, and J. Q. Lu, J. Magn. Magn. Mater. **193**, 136 (1999).
[34]S. Uba, L. Uba, A. N. Yaresko, A. Ya Perlov, V. N. Antonov, and R. Gontarz, Phys. Rev. B **53**, 6526 (1996).
[35]C. Jing, S. X. Cao, and J. C. Zhang, Phys. Rev. B **68**, 224407 (2003).
[36]W. Park, D. V. Baxter, S. Steenwyk, I. Moraru, W. P. Pratt, Jr., and J. Bass, Phys. Rev. B **62**, 1178 (2000).
[37]U. Nowak, U. Rüdiger, P. Fumagalli, and G. Güntherodt, Phys. Rev. B **54**, 13017 (1996).
[38]U. Nowak, J. Heimel, T. Kleinefeld, and D. Weller, Phys. Rev. B **56**, 8143 (1997).
[39]M. Hehn, S. Padovani, K. Ounadjela, and J. P. Bucher, Phys. Rev. B **54**, 3428 (1996).
[40]S. Ferrer, J. Alvarez, E. Lundgren, X. Torrelles, P. Fajardo, and F. Boscherini, Phys. Rev. B **56**, 9848 (1997).
[41]N. Nakajima *et al.*, Phys. Rev. Lett. **81**, 5229 (1998).